

Energy-efficient Irregular Repetition Slotted ALOHA for IoT Satellite Systems

Estefanía Recayte*, Tijana Devaja†, Dejan Vukobratovic†

*Institute of Communications and Navigation, German Aerospace Center (DLR), Weßling, Germany.

†Department of Power, Electronics and Communications Engineering, University of Novi Sad, Novi Sad, Serbia.

Abstract—There is an urgent need to enhance random access schemes, specifically designed to support massive Internet of things communications in satellite systems. These scenarios are limited by two key factors: the lifespan of device batteries and the scarcity of satellite resources. To overcome such limitations, we propose to apply per replica power diversity to irregular repetition slotted ALOHA protocol. We evaluate the protocol performance in terms of energy and spectral efficiency. We provide an asymptotic analysis to track the decoding process at the satellite, and complement our study by means of simulations to explore the finite frame length case. In both settings, the proposed scheme triggers significant and promising improvements with respect to the state of the art.

I. INTRODUCTION

Satellite communications (Satcom) play a crucial role in the context of Internet of Things (IoT), especially when terrestrial infrastructure is unavailable such as in remote areas. Satcom provides reliable connectivity, overcoming geographical limitations and facilitating the deployment of IoT applications in different environments [1]. In particular, starting from Release 17 [2], Satcom has become part of the 3GPP communications ecosystem, emphasizing its importance in the advancement towards sixth generation (6G) technology. In scenarios where connectivity has to be provided to a massive number of devices that generate traffic sporadically, enhancing the traditional random access schemes in communication systems becomes crucial to address the battery limitations inherent in IoT devices. From this standpoint, finding novel solutions for energy- and spectrum-efficient satellite communications is critical.

In the context of massive IoT satellite communications, there is an ongoing focus on enhancing the design of grant-free random access protocols, where multiple devices share a common channel and transmit in an uncoordinated manner. Versions of the well-known ALOHA protocol now dominate commercial applications (such as LoRa [3] and Sigfox [4]) and industry standards (including NB-IoT and LTE-M [5]). In parallel to this, modern random access protocol design concepts have demonstrated their ability to offer competitive solutions in terms of spectral efficiency with respect to grant-based solutions [6]–[8]. A relevant example can be found in

the case of irregular repetition slotted ALOHA (IRSA) [9]. In IRSA, nodes independently transmit a random number of copies of their data packets within a predefined frame and successive interference cancellation (SIC) algorithm is applied to decode information at the receiver end. Thanks to the enhancement over existing protocols, IRSA has become part of the standard DVB-RCS2.

Researchers are increasingly directing their attention towards enhancing energy efficiency in IoT networks within the domain of green communications [10]. The energy efficiency performance of the IRSA protocol was first studied in [11] considering the optimization of both transmit power and maximum replica repetition rate. In [12], a power optimization problem was examined for contention resolution diversity slotted ALOHA (CRDSA), a special case of IRSA in which all users transmit the same number of replicas. In such work, the authors prioritize enhancing throughput, yet neglecting the crucial aspect of energy efficiency. In [13], the idea of per-replica power diversity has been investigated for a fixed level of energy consumption, assuming each node transmit a fixed number of two replicas at two different power levels. The IRSA protocol was evaluated under non-orthogonal multiple access (NOMA) [14] where the satellite fixes the transmission power for each IoT device. An open loop power control solution where each terminal transmits at a different power was studied for the CRDSA protocol in [15].

In contrast to the existing literature, our aim is to enhance energy and spectral efficiency in a satellite random access scenario. Specifically, we propose to apply replica power diversity to the IRSA protocol, allowing replicas of the same IoT device to be transmitted at different power levels. We evaluate how this power levels shall be derived. We formulate an asymptotic analysis to monitor the performance of the SIC decoding process. Our study is complemented by simulations to explore the practical implications of finite frame lengths. We compare our results with both the original scheme [9] and the throughput optimized scheme studied in [12], focusing on energy consumption and spectral efficiency.

II. SYSTEM MODEL

We explore a scenario in which m uncoordinated IoT devices (*users* or *nodes*) communicate with a satellite following a time-slotted multiple access protocol. Each packet is

E. Recayte acknowledges the financial support by the Federal Ministry of Education and Research of Germany in the programme of “Souverän. Digital. Vernetzt.” Joint project 6G-RIC, project identification number: 16KISK022.

transmitted in a single time slot, and a medium access control (MAC) frame is composed by a sequence of n consecutive time slots.

Following the IRSA protocol, each user sends a number of packet copies, referred to as *replicas*, determined by a specific probability distribution. The probability that a node transmits r replicas is denoted as Λ_r . Following the common notation [7], we will make use of the polynomial formulation as $\Lambda(x) = \sum_r \Lambda_r x^r$.

All replicas sent by a user are randomly placed across r distinct time slots among the n available, following a uniform distribution. Each replica's header contains information about the slot indexes where its copies are located. We denote with \bar{r} the average number of replica repetitions of the scheme, i.e.

$$\bar{r} = \sum_{r=2}^{r_{\max}} r \Lambda_r$$

where r_{\max} is the maximum number of copies a user can send within a frame, and we assume that at least two replicas transmitted per user [9]. The normalized offered traffic (or channel traffic), denoted with G , is thus defined as

$$G = \frac{m}{n} \quad [\text{packets/slot}]. \quad (1)$$

We operate under the assumption that each IoT device is bound to a peak power constraint,¹ which is denoted by P . We assume that IoT devices have access to two power levels, both expressed as fractions of the peak power: the *weak* power level and the *strong* power level. User k transmits a replica in slot j with probability $p \in (0, 1)$ at weak power level and with probability $(1 - p)$ at strong power level, that is

$$P_{(k,j)} = \begin{cases} \alpha P & \text{with probability } p \\ (1 - \alpha)P & \text{with probability } (1 - p) \end{cases}$$

where $P_{(k,j)}$ denotes the replica sent by user k in slot j , while α is the *power coefficient*, satisfying the condition $0 < \alpha \leq 1/2$.

In this scenario, we operate under the assumption of an ideal channel and for simplicity we assume that the transmitter power matches the received power as in [14]. We also assume that IoT nodes transmit each replica at a rate R . This rate is set so that a collision-free packet transmitted at lower power level, i.e. at αP , is successfully decoded. Assuming we use capacity achieving codes and sufficiently long packets, we have that $R = \log_2 \left(1 + \frac{\alpha P}{N} \right)$, where N denotes the noise power.

Satellite receiver

We consider *capture effect* at the satellite, where the strongest signal can be successfully decoded, even in the presence of interference from a weaker signal generated by another user in the same slot. Formally, the capture effect occurs when the signal-to-interference and noise ratio (SINR) exceeds a predefined threshold denoted as γ . In general, the

¹This assumption is based on practical considerations, including factors such as amplifier performance and spectrum usage regulations.

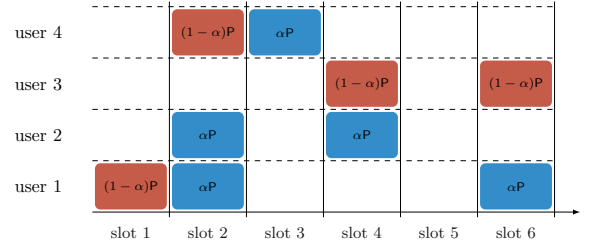


Fig. 1. Transmission over a MAC frame of $n = 6$ slots and with $m = 5$ users. Colors represent the transmission power levels, i.e. αP and $(1 - \alpha)P$.

SINR $\Gamma_{(k,j)}$, of the replica transmitted by user k in slot j can be expressed as

$$\Gamma_{(k,j)} = \frac{P_{(k,j)}}{N + \sum_{u \neq k} P_{(u,j)}} \quad (2)$$

where $P_{(k,j)}$ and $P_{(u,j)}$, according to the proposed scheme, take values in $\{\alpha P, (1 - \alpha)P\}$.

Next, we provide an explanation of the receiver's implementation of the SIC algorithm.

III. DECODING PROCEDURE

Capture effect

During the decoding, a slot containing *two* colliding replicas captures the strongest replicas when its SINR exceeds the capture threshold γ . Given that the rate has been determined, we set the decoding threshold to

$$\gamma = \frac{\alpha P}{N}. \quad (3)$$

Referring to (2), it is important to highlight that the strongest replica (k,j) can be captured even when it collides with a weaker replica. This situation can be expressed as $\Gamma_{(k,j)} \geq \gamma$ and, substituting the corresponding values, we have

$$\frac{(1 - \alpha)P}{N + \alpha P} \geq \frac{\alpha P}{N}. \quad (4)$$

Inequality (4) imposes a condition on the choice of the value of the power splitting coefficient α . If we solve for α we obtain

$$\alpha \leq \frac{\sqrt{N(1 + P)} - N}{P}. \quad (5)$$

When the splitting power coefficient α is chosen such that (5) holds, then the transmission rate of the scheme is maximized.

Example 1. Let us assume that N is unitary, and consider that the maximal signal-to-noise ratio (SNR) of the nodes can achieve if performing at peak power is $P/N = 10$ dB. Solving for α in (5), we find that when $\alpha = 0.2317$, the satellite captures the strongest replica in a slot with a collision involving two replicas. Using inequality (5), we can compute the value of α for different values of P and N .

Successive interference cancellation

The decoding process is based on SIC [9], which starts at the receiver slot-by-slot, after the frame has been stored in the buffer. The satellite processes the entire frame, and whenever the condition $\Gamma_{(k,j)} \geq \gamma$ is met, the replica of user k is successfully decoded. The receiver is then able to extract the position information of the sibling replicas from the header. Ideal interference cancellation is performed to both the decoded replica and its copies. This may in turn render other packets decodable, having lowered the interference level they experience. The scanning of the entire frame may be performed multiple times. The decoder stops the process when one of the following two conditions is met: either all users have been successfully solved, or the $\Gamma_{(k,j)}$ for each remaining (k, j) is below the decoding threshold γ .

An example transmission scheme is shown in Fig. 1. When γ is set as in eq. (3), the receiver is able to recover all replicas due to power diversity and SIC.

IV. ASYMPTOTIC ANALYSIS

Examining the performance of the power diversity scheme within finite-length frames is challenging, mainly due to the complex SIC process involved [9], [16]. To have insights on the behavior of the proposed protocol, we relax the time constraint in the following analysis. We assume to have users placing their replicas over an infinite frame duration. Thus, we can apply density evolution (DE), a powerful tool used in coding theory. DE allows to analyze and predict the asymptotic performance of the iterative decoding process.

DE involves the iterative computation of two probabilities, denoted with $q_{(i)}$ and $p_{(i)}$ for a specific channel load G . The algorithm outputs the packet loss rate for the given G . The value of $q_{(i)}$ represents the probability that a user, randomly selected during the i -th step of the SIC process, is not decoded during the iteration. Similarly, the value of $p_{(i)}$ represents the probability that a slot, randomly chosen during the i -th iteration of the SIC process, remains unresolved, i.e., it has two or more colliding packets at the end of the iteration.

Evaluation of $q_{(i)}$

We can express the probability that a user remains unresolved at iteration i , $q_{(i)}$, if none of the replicas sent by the user was revealed during the previous iteration, i.e. $i-1$, with a probability $p_{(i-1)}$. Consequently, it follows that

$$q_{(i)} = \sum_{r=1}^{r_{\max}} \lambda_r p_{(i-1)}^{r-1}.$$

Evaluation of $p_{(i)}$

The probability that a slot remains unsolved at the i -th iteration, $p_{(i)}$, relies on the probability π_t of having t replicas colliding within the slot, all of which remain unsolved with probability $p_{(i)}^{[t]}$. For each possible value of t , we can express this probability as

$$p_{(i)} = \sum_{t=1}^{\infty} \pi_t p_{(i)}^{[t]}. \quad (6)$$

Asymptotically, π_t is approximated to [9]

$$\pi_t \approx \frac{(\bar{r}G)^{t-1}}{(t-1)!} e^{-\bar{r}G}. \quad (7)$$

For $t = 1$ we have that $p_{(i)}^{[1]} = 0$, since the decoder can always decode collision-free replica. For $t > 1$, the probability that none of the t replicas are successfully resolved, $p_{(i)}^{[t]}$, at the i -th iteration can be calculated from the complementary event - when at least one replica is decoded. To this aim, observe that a reference replica is decoded during the SIC process in only two occasions. The first occasion is when the replica is interference-free. This condition occurs when the SIC algorithm cancels all replicas except one from the slot or when the packet was originally sent over a singleton slot. The second occasion occurs when all replicas, except for two (the reference and another), have been removed from the slot and, the reference replica is transmitted at a strong power level while the other is transmitted at a weak power level. The probability of successful decoding, denoted as $\Pr\{D\}$, can be written considering the two events as

$$\Pr\{D\} = (1 - q_{(i)})^{t-1} + p(p-1)(t-1)q_{(i)}(1 - q_{(i)})^{t-2}, \quad (8)$$

where $(1 - q_{(i)})^{t-x}$ represents the scenario where all but x replicas have been cancelled in the slot due to the SIC process. The term $p(p-1)$ denotes the probability that one replica is transmitted at the strong power level, while the other at weak power level. Lastly, the term $(t-1)q_{(i)}$ denotes all possible combination of $t-2$ replicas remaining not cancelled. From Equation (8), we can write

$$\begin{aligned} p_{(i)}^{[t]} &= 1 - \Pr\{D\} \\ &= 1 - \left[(1 - q_{(i)})^{t-1} + p(p-1)(t-1)q_{(i)}(1 - q_{(i)})^{t-2} \right] \end{aligned} \quad (9)$$

When we insert (7) and (9) into (6), we can write

$$\begin{aligned} p_{(i)} &= e^{-\bar{r}G} \sum_{t=1}^{\infty} \frac{(\bar{r}G)^{t-1}}{(t-1)!} - e^{-\bar{r}G} \sum_t \frac{[\bar{r}G(1 - q_{(i)})]^{t-1}}{(t-1)!} \\ &\quad - p(1-p)\bar{r}Gq_{(i)} e^{-\bar{r}G} \sum_t \frac{[\bar{r}G(1 - q_{(i)})]^{t-2}}{(t-2)!}. \end{aligned} \quad (10)$$

Noting that $\sum_t x^t/t! = e^x$, (10) can be written as

$$\begin{aligned} p_{(i)} &= 1 - e^{\bar{r}G(1 - q_{(i)})} e^{-\bar{r}G} - p(1-p)\bar{r}Gq_{(i)} e^{\bar{r}G(1 - q_{(i)})} e^{-\bar{r}G} \\ &= 1 - e^{-\bar{r}Gq_{(i)}} (1 + p(1-p)\bar{r}Gq_{(i)}). \end{aligned}$$

It is worth noting that the scenario explored in [13] represents a special case within the broader framework of the currently proposed scheme. In particular, in that work each user transmits a fixed number of replicas, denoted as $\bar{r} = 2$ where always one replica is transmitted at the strong power level, and the other at weak power level.

DE execution

The performance of the SIC process for the scheme, in the asymptotic case can be determined leaning on $q_{(i)}$ and $p_{(i)}$. More precisely, iterating for a total of l_{\max} times, we have

$$\begin{cases} q_{(i)} = \sum_{r=1}^{r_{\max}} \lambda_r p_{(i-1)}^{r-1}, \\ p_{(i)} = 1 - e^{-\bar{r} G q_{(i)}} (1 + p(1-p) \bar{r} G q_{(i)}). \end{cases} \quad (11)$$

The initial conditions are set to one, $q_{(0)} = p_{(0)} = 1$. After l_{\max} iterations, the value of $p_{(i=l_{\max})}$ represents the probability that a replica is not decoded. The packet loss rate is given by $\text{PLR}(G) = \sum_{r=2}^{r_{\max}} \lambda_r p_{(l_{\max})}^r$ [9].

The DE algorithm allows us to calculate the maximum load G^* that the scheme can support, while ensuring that SIC converges to a vanishing small error probability [9], i.e. $p_{(l_{\max})} \rightarrow 0$ and consequently $\text{PLR}(G^*) \rightarrow 0$. The scheme's performance in the asymptotic domain strictly depends on the replicas distribution $\{\Lambda_r\}$ and the probability p of transmitting replicas at weak power level or strong power level, i.e. $1-p$. These two probabilities also determine the average energy consumed per node. Next, we evaluate the proposed scheme in terms of energy and aggregate spectral efficiency.

SPECTRAL AND ENERGY EFFICIENCY

Aggregate spectral efficiency

The aggregate spectral efficiency S measures how efficiently the protocol uses the available spectrum to transmit data. This metric is crucial in system design, since in the case of random access it allows to understand how many devices can effectively share the channel. For a given channel load G , S is calculated as the average number of information bits successfully delivered per unit of time and bandwidth, that is

$$S = R \cdot (1 - \text{PLR}(G)) \cdot G \quad [\text{bit/s/Hz}]$$

In the context of asymptotic frame duration, we can determine the maximum achievable aggregate spectral efficiency, denoted as S^* , noting that when the frame is sufficiently long then PLR is vanishing small. Thus, S^* is determined by the maximum achievable rate G^* so that

$$S^* = R \cdot G^* \quad [\text{bit/s/Hz}].$$

Energy

If we denote the packet duration with T , the average energy consumption E of a node can be calculated as the product of the expected number of replicas, determined by the distribution, and the average power consumed per replica. The relationship can be expressed as follows

$$\begin{aligned} E &= \sum_{r=2}^{r_{\max}} r \Lambda_r [p \alpha P + (1-p)(1-\alpha)P] T \quad (12) \\ &= \bar{r} [p \alpha + (1-p)(1-\alpha)] P T \quad [\text{J}]. \end{aligned}$$

Given that α is determined in (5), the energy consumed per user can be adjusted in the design by choosing both the repetition replica distribution and the probability of transmitting replicas at either the weak power or the strongest power.

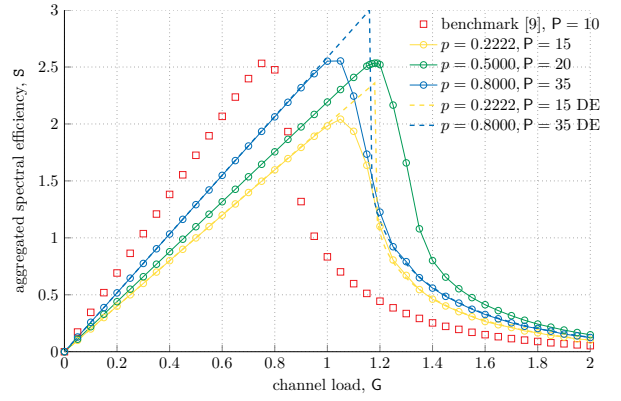


Fig. 2. Aggregate spectral efficiency S as a function of the channel load G for benchmark [9] ($p = 1$, SNR = 10 dB) and our scheme for different peak power P and power distribution p . Simulations with frames of length $n = 200$ are represented with marker curves, while dashed indicate asymptotic behavior. The average energy consumption $\eta = 29.79$ for all schemes.

Another interesting metric to evaluate in this context is the average energy consumed per successfully transmitted bit per unit time and unit bandwidth. We denote this quantity as η , which represents energy efficiency

$$\eta = \frac{\bar{r} [p \alpha + (1-p)(1-\alpha)] P T}{R \cdot (1 - \text{PLR}(G)) \cdot G} \quad [\text{J/bit/s/Hz}].$$

V. NUMERICAL RESULTS AND DISCUSSION

In this section, the numerical results obtained for the proposed scheme are presented. The scheme was evaluated by simulations for the finite frame length and analytically for the case of infinite frame length. Our main focus is to compare our work to the benchmark IRSA scheme introduced in [9] and with the approach in [12], where the authors concentrate on optimizing power distribution to maximize throughput.

For simplicity, we set unitary packet duration and noise power in all the results presented. In this way we focus on the energy consumed per packet duration and neglect the unit of measure (Joules).

Aggregate spectral efficiency

In our initial scenario, we evaluate the aggregate spectral efficiency in the case of a finite frame length of $n = 200$ slots (curves with markers) obtained through simulations and for the asymptotic behavior derived from the analysis (dashed curves). The number of users per slot is determined in (1). As a reference benchmark, we use the distribution $\Lambda(x) = 0.5102x^2 + 0.4898x^4$ [9] in which all replicas are transmitted with SNR= 10 dB, leading to an average energy consumption per node $E = 29.796$. In our scheme, we fix the replica distribution and the energy consumption per node E , while varying the power P and the corresponding probability p from (12), and α (5). In this context, we illustrate the aggregate spectral efficiency S as a function of the channel load G in Fig. 2. Red marks indicate the benchmark results [9], while other colors denote the results for the proposed scheme

TABLE I
SYSTEM PARAMETERS FOR $E = 29.796$

P	α	γ	p	R
15	0.2000	3.0000	0.2222	2.0000
20	0.1791	3.5826	0.5000	2.1962
25	0.1640	4.0990	0.6488	2.3502
30	0.1523	4.5678	0.7396	2.4771
35	0.1424	5.0000	0.8000	2.5850

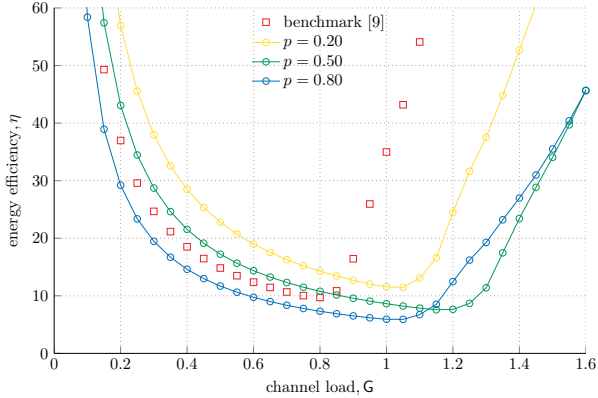


Fig. 3. Energy efficiency η as function of channel load G . Replica distribution is set to $\Lambda = 0.5102x^2 + 0.4898x^4$. Red curve represents the benchmark [9] while other colors represent different values of power distribution p .

using parameters detailed in Table V. It can be observed that at low and medium channel loads, roughly up to $G = 0.8$, the benchmark demonstrates superior performance. At these channel load values, all schemes exhibit similar throughput behavior. However, the benchmark scheme transmits at a higher rate compared to the proposed scheme, leading to a higher aggregate spectral efficiency. Conversely, at higher channel loads, all presented configurations outperform the existing technique. In this case, the proposed scheme achieves higher throughput values, compensating for the lower rate, thereby outperforming the benchmark. In particular, for the same energy consumption per user, our scheme achieves a higher spectral efficiency at high channel load, which means transmitting more information bits per s/Hz and the capacity to support a higher number of devices. These insights are fundamental importance when designing an IoT network. The different behavior among the configurations is attributed both to the influence of the power probability distribution, determined by p and the effect of the transmission rate R . The variation of p directly influences the SIC decoding algorithm and, consequently, the throughput achieved at a given load. In turn, the rate directly affects the spectral efficiency.

Finally, the dashed curves represent the results obtained through the density evolution analysis presented in Sec. IV for the selected setups. These curves show the maximum achievable S^* for the configuration, given that users are placing their replicas in a not finite frame.

Energy efficiency

To evaluate the energy efficiency η of the scheme, we consider again the replica distribution $\Lambda(x) = 0.5102x^2 + 0.4898x^4$

and different values of the power probability p . The frame duration is set to $n = 200$ slots. A SNR = 10 dB is assumed when replicas would be transmitted at peak power and, unitary noise power and, as a consequence, $\alpha = 0.2317$ from (5). In Fig. 3 the energy efficiency is plotted against the channel load for different values of the probability p . Transmitting 80% of the replicas at power αP outperforms for every channel load the benchmark IRSA scheme which does not consider power splitting. Indeed, the proposed scheme can achieve an energy efficiency $\eta = 6.41$ against of a $\eta = 9.72$ of the traditional method. Instead, when $p = 0.20$ or $p = 0.50$ the scheme still performing better than the benchmark for high values of channel load, $G > 0.85$ user/slot.

The proposed scheme, when considering a value of $p = 0.80$, consistently exhibits a gain for loads $G \leq 0.8$, resulting in a substantial 22% reduction in average energy consumption per successful bit transmission per s/Hz when compared to the benchmark. This enhancement becomes notably more significant as the load surpasses $G > 0.8$, reaching for example at $G = 1$ an impressive 83% reduction in energy consumption.

In other words, by correctly choosing p the power splitting scheme allows at any given channel load to spend less energy in average for every successful transmitted information per s/Hz. This metric is also an essential insight at the moment of designing of the communication network, for instance to evaluate the duration of the battery node in IoT Satcom.

Energy consumption versus maximum spectral efficiency

In our last scenario, we consider the average energy required per user to achieve a target specific spectral efficiency in the asymptotic domain. We explore two distinct approaches. In the first approach, we maintain a fixed power distribution, specifically $p = 1/2$. Meanwhile, we consider different replica distributions in the form $\Lambda(x) = ax^2 + (1 - a)x^3$ where we examine different configurations considering values of a within the interval $[0, 1]$ in increments of 0.05. Changing the value of a implies changing the average number of transmitted replicas per user. Through density evolution analysis, as outlined in (11), we derive the maximum achievable spectral efficiency S^* and the corresponding average energy consumption per node. In the second approach, we keep the replica distribution constant $\Lambda(x) = 0.65x^2 + 0.33x^3 + 0.02x^4$ while varying the power distribution p in the interval of $[0, 1]$ in increments of 0.05. So, we are varying the probability of transmitting replicas at weak (strong) power. Excluding the benchmark points, each of the points plotted in this figure represents the best spectral efficiency-energy pair consumed for a different configuration of the proposed scheme. In all cases, SNR = 10 dB and $\alpha = 0.2317$.

In Fig. 4 the average energy consumed E versus the maximum spectral efficiency S^* for different system configurations is plotted. The red markers in the figure represent some operational points from [12] where power optimization is employed to enhance throughput. All the specific operational points detailed in [12], including the maximum channel load G^* , maximum spectral efficiency S^* , average replicas trans-

TABLE II
SYSTEM RESULTS FROM BENCHMARK IN [12]

G^*	S^*	\bar{r}	E
0.82	0.82	5	12.499
1.04	1.04	4	9.999
1.06	1.06	5	74.891
1.18	1.18	3	7.499
1.68	1.68	2	17.017
1.33	1.33	4	38.790
1.58	1.58	3	29.776

mitted per node \bar{r} and energy consumption E, are presented in Table II. It is important to note that, in all these configurations, G^* equals S^* , due to the fact that the transmission rate is consistently set at $R = 1$. This condition is determined by the minimum transmitted power $P = 0$ dB used in [12].

The results demonstrate that operational points in our scheme are significantly more efficient in terms of both spectral efficiency and average energy consumption when compared to the scheme outlined in [12]. In fact, for a given average energy consumption, our scheme achieves a significantly higher level of spectral efficiency. While the benchmark consumes nearly $E = 10$ and achieves a spectral efficiency of $S^* = 1.04$ bit/s/Hz, our approach allows a transmission of $S^* = 2.16$ bit/s/Hz with an average consumption of $E = 9.86$.

It can be observed that green circles for a given spectral efficiency value, allows the system to operate at two different levels of average energy consumption. This can be explained by (8), where, when $p = y$ with $y < 1/2$, and when $p = 1 - y$, the result of $p(1-p)$ is equal in both cases, leading to the same spectral efficiency. However, when $p = 1 - y$, the protocol consumes less energy compared to when $p = y$ because, in the former case, most replicas are transmitted at weak power.

This symmetrical behavior is not present in the approach of varying the replica distribution. By varying the distribution of replicas, the expected number of replicas transmitted per user also varies, which has a direct impact on the average energy and the maximum achievable spectral efficiency in the asymptotic case. For configurations in which the value $a \in \{0.25, 0.50\}$ the DE obtains the same maximum spectral efficiency point of $S^* = 2.214$ bit/s/Hz. Note that larger is a and less energy per node is consumed.

VI. CONCLUSIONS

In the context of an IoT satellite system, we proposed enhancing energy and spectral efficiency by modifying the IRSA protocol to enable devices to transmit replicas at two power levels. Our results highlight the substantial gains of the proposed approach, which we compared with established benchmarks. We have shown that per-replica diversity applied to IRSA protocol leads to a notably higher level of spectral efficiency for a given energy consumption. Our results reveal a significant reduction in average energy consumption compared to current schemes which can reach over 80%, all while improving the efficient utilization of available bandwidth.

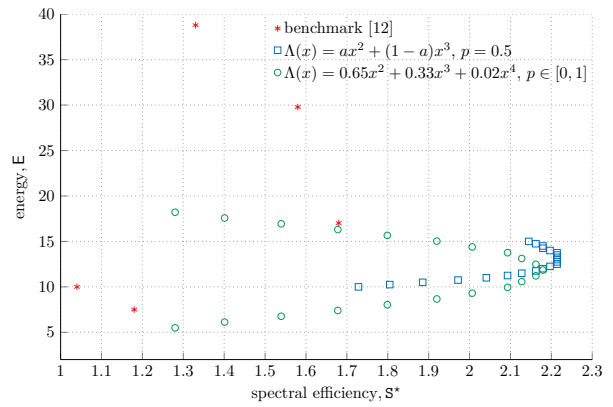


Fig. 4. Average energy consumption E versus the maximum achievable spectral efficiency S^* for the scheme, and benchmark [12]. Square markers are obtained by fixing the probability p and varying the replica distribution while round markers are obtained by varying the probability.

REFERENCES

- [1] M. De Sanctis, E. Cianca, G. Araniti, I. Bisio, and R. Prasad, "Satellite communications supporting internet of remote things," *IEEE Internet of Things Journal*, vol. 3, no. 1, pp. 113–123, 2016.
- [2] 3GPP, "21.917: Release 17 description; summary of rel-17 work items : Technical report (tr)," Tech. Rep., 2021.
- [3] LoRaWAN, "LoRa Alliance Tech. Committee," Oct. 2017.
- [4] SIGFOX, "The Global Communications Service Provider for the Internet of Things," Feb. 2021.
- [5] Y.-P. E. Wang, X. Lin, A. Adhikary, A. Grovlen, Y. Sui, Y. Blankenship, J. Bergman, and H. S. Razaghi, "A Primer on 3GPP Narrowband Internet of Things," *IEEE Commun. Mag.*, vol. 55, no. 3, pp. 117–123, 2017.
- [6] M. Berlioli, G. Cocco, G. Liva, and A. Munari, *Modern Random Access Protocols*. NOW Publisher, 2016.
- [7] E. Paolini, G. Liva, and M. Chiani, "Coded Slotted ALOHA: A Graph-Based Method for Uncoordinated Multiple Access," *IEEE Trans. Inf. Theory*, vol. 61, no. 12, pp. 6815–6832, 2015.
- [8] C. Stefanovic and P. Popovski, "ALOHA Random Access that Operates as a Rateless Code," *IEEE Trans. Commun.*, vol. 61, no. 11, pp. 4653–4662, 2013.
- [9] G. Liva, "Graph-Based Analysis and Optimization of Contention Resolution Diversity Slotted ALOHA," *IEEE Trans. Commun.*, vol. 59, no. 2, pp. 477–487, 2011.
- [10] K. Wang, Y. Wang, Y. Sun, S. Guo, and J. Wu, "Green industrial Internet of Things Architecture: An Energy-Efficient Perspective," *IEEE Commun. Mag.*, vol. 54, no. 12, pp. 48–54, 2016.
- [11] Z. Chen, Y. Feng, Z. Tian, Y. Jia, M. Wang, and T. Q. S. Quek, "Energy Efficiency Optimization for Irregular Repetition Slotted ALOHA-Based Massive Access," *IEEE Wireless Commun. Lett.*, vol. 11, no. 5, pp. 982–986, 2022.
- [12] S. Alvi, S. Durrani, and X. Zhou, "Enhancing CRDSA With Transmit Power Diversity for Machine-Type Communication," *IEEE Trans. Veh. Technol.*, vol. 67, no. 8, pp. 7790–7794, 2018.
- [13] E. Recayte and F. Clazzer, "Per-Replica Power Diversity in Grant-Free Multiple Access: Design and Performance Evaluation," in *2023 IEEE Globecom*, 2023.
- [14] X. Shao, Z. Sun, M. Yang, S. Gu, and Q. Guo, "NOMA-Based Irregular Repetition Slotted ALOHA for Satellite Networks," *IEEE Communications Letters*, vol. 23, no. 4, pp. 624–627, 2019.
- [15] A. Mengali, R. De Gaudenzi, and P.-D. Arapoglou, "Enhancing the physical layer of contention resolution diversity slotted aloha," *IEEE Transactions on Communications*, vol. 65, no. 10, pp. 4295–4308, 2017.
- [16] M. Ivanov, F. Brännström, A. Graell i Amat, and P. Popovski, "Error Floor Analysis of Coded Slotted ALOHA Over Packet Erasure Channels," *IEEE Commun. Lett.*, vol. 19, no. 3, pp. 419–422, 2015.